Available online at www.sciencedirect.com
ScienceDirect
Polymer 48 (2007) 7156–7162
polymer
www.elsevier.com/locate/polymer

Synthesis and characterization of photorefractive polymer based on chemically hybridized CdS–PVK nanocomposite with a new azo chromophore

Desheng Jiang [a], Liyun Ding [a,*], Jun Huang [a], Erdan Gu [a], Liren Liu [b], Zhifang Chai [b], De'an Liu [b]

[a] *Key Laboratory of Fiber Optic Sensing Technology and Information Processing, Ministry of Education, Wuhan University of Technology, Wuhan 430070, PR China*
[b] *Laboratory of Information Optics, Shanghai Institute of Optics and Fine Mechanics, The Chinese Academy of Sciences, Shanghai 201800, PR China*

Received 25 January 2007; received in revised form 7 September 2007; accepted 13 September 2007
Available online 26 September 2007

Abstract

We report an organic/inorganic polymer composite based on the chemically hybridized photoconductor CdS–PVK nanocomposite doped with a new second-order optically nonlinear chromophore 1-*n*-butoxy-2-methyl-(4-*p*-nitrophenylazo)benzene (BMNPAB) and plasticizer 9-ethylcarbazole (ECZ) to manifest a photorefractive (PR) effect. A detailed description of the synthesis and characterization of BMNPAB is presented. The poled film including PVK–10-CdS nanocomposite and BMNPAB exhibits a high second harmonic generation (SHG) coefficient of 31 pm/V. The photoconductivity of PVK–CdS nanocomposite also was studied here. Two-beam coupling experiment clearly indicated an asymmetric optical energy exchange between two beams on the polymer composite at zero electrical field, and the two-beam coupling gain of 50.0 cm^{-1} and diffraction efficiency of 4.2% were obtained at 647.1 nm wavelength.

Keywords: Photorefractive polymer; Chemically hybridized CdS–PVK nanocomposite; 1-*n*-Butoxy-2-methyl-(4-*p*-nitrophenylazo)benzene

1. Introduction

Photorefractive polymeric materials have been extensively studied because of their large optical nonlinearities, low dielectric constants, ease of preparation and low cost [1–4]. However, the main obstacle for the practical use of PR polymeric materials is the necessity to apply a relatively large DC field, E_0, to insure effective recording of holographic gratings with high diffraction efficiency. Most of photorefractive polymeric materials require the high electric fields in the range of 50–100 V/μm. Several approaches have been proposed to reduce E_0, including the substitution of the traditional organic photosensitizers (e.g. 2,4,7-trinotro-9-fluorenone (TNF) or C_{60}) with inorganic nanocrystals. Nanocomposites containing inorganic quantum dots dispersed in a polymer matrix exhibit increased photogeneration efficiency, broadened spectrally tunable photoresponse and enhanced carrier mobility, so the hybrid organic/inorganic materials with semiconductor nanoparticles have emerged as a novel class of photorefractive materials in recent years [5–8]. Nevertheless, a major limitation of organic/inorganic materials is the compatibility between the polymers and semiconductor nanoparticles due to phase separation. The chemically hybridized CdS–poly(*N*-vinylcarbazole) (PVK) nanocomposites introduced by Wang et al. [9,10] could be expected to overcome this weakness, which also exhibit the significant enhancement of photoconductivity as compared to CdS/PVK nanoblends owing to the improved

* Corresponding author. Tel.: +86 27 87651850x8005; fax: +86 27 87665287.
E-mail address: dlyw@whut.edu.cn (L. Ding).

0032-3861/$ - see front matter © 2007 Elsevier Ltd. All rights reserved.
doi:10.1016/j.polymer.2007.09.030

interface quality between CdS and PVK. Besides the photosensitizers, the NLO chromophore plays a key role in PR polymeric materials because it contributes spatially modulated electro-optic and birefringent components to the grating, with the latter being due to the reorientation of the mobile chromophore in the host matrix. The azo dyes are well-known electro-optic chromophores and exhibit high EO coefficient. For PR effect, azo-dye derivatives have been the molecule of choice, since upon resonant illumination with linearly polarized light, they undergo a cycle of *trans–cis* isomerizations that cause the dye to orient perpendicular to the incident (polarized) light direction, thereby producing large changes in optical birefringence.

In this paper, we report on the synthesis and characterization of a new NLO chromophore 1-*n*-butoxy-2-methyl-(4-*p*-nitrophenylazo)benzene (BMNPAB), and photorefractive performance of the polymer composite consisting of the chemically hybridized CdS–PVK nanocomposite, the chromophore BMNPAB and the plasticizer 9-ethylcarbazole (ECZ). We measured the nonlinear optical property of the poled film including PVK–10-CdS nanocomposite and BMNPAB by second harmonic generation (SHG) used the Maker fringe technique. Since the photogeneration of charge carriers and their subsequent migration by diffusion or drift in an electric field play a key role in determining the magnitude and speed of the PR response, photoconductivity of chemically hybridized CdS–PVK nanocomposite is also studied here.

2. Experimental

2.1. Materials

All chemicals, poly(*N*-vinylcarbazole) (PVK) (secondary standard, ACROS), 9-ethylcarbazole (ECZ) (ACROS), nitrobenzene, *p*-nitroaniline, sodium nitrous acid, sodium *n*-dodecylphenyl sulfonate, cadmium chloride, tetrahydrofuran (THF), hydrochloric acid (37%), acetic anhydride, methanol, cadmium acetate dihydrate and sodium sulfide were used as purchased without further purification.

The chemically hybridized CdS–PVK nanocomposites were synthesized with a similar procedure as described in the literature [9]. The preparation included the sulfonation of PVK, the preparation of the precursor $PVK(SO_3)_2Cd$ and the in situ formation of CdS–PVK nanocomposite. In this study, the synthesized PVK–10-CdS nanocomposite sample with the molar ratio of CdS to PVK being 1:80 was chosen for photorefractive device.

2.2. Synthesis of 1-n-butoxy-2-methyl-(4-p-nitrophenylazo)benzene

p-Nitroaniline (1.32 g, 0.05 mol) was dissolved in a mixture of 18 ml hydrochloric acid (37%) and 40 ml water, and it was stirred for 1 h at 5 °C. When reaction temperature was kept under 5 °C, 3.8 g (0.05 mol) of sodium nitrous acid in 13 ml water was added to the above solution. Then a small quantity of carbamide was added to remove redundant sodium nitrous acid. *o*-Cresol (5.41 g, 0.05 mol) dissolved in 40 mL lye (the mixture of 10% NaOH solution and 10% $NaCO_3$ solution with volume ratio 1:2) was added dropwise to this reaction solution, yielding an opaque reddish orange solution. After stirring the mixture for 24 h under the temperature of 5 °C, the carmine phase was isolated and aqueous phase was extracted several times with ethanol. The raw product 2-methyl-(4-*p*-nitrophenylazo)phenol (MNPAP) was dried in vacuum and purified by column chromatography with methanol as diluent. Yield = 7.97 g (62%). IR (in KBr) ν/cm^{-1}: 3500 (–OH), 1595 (N=N), 3106 (ar. C–H), 1510, 1255 (ar. C–N), 845 (N–O).

MNPAP, 7.71 g (0.03 mol) and *n*-butyl bromide, 4.08 g (0.03 mol) were circumfluxed in acetone for 4 h and it was kept alkaline throughout the reaction time by adding additional amounts of cold 10% NaOH solution if needed. After the reaction was completed, acetic ether was added to make the mixture acidic and kept overnight in fridge. The precipitated 1-*n*-butoxy-2-methyl-(4-*p*-nitrophenylazo)benzene (BMNPAB) (Scheme 1) was filtered, washed with water and dried. Yield = 8.17 g (87%). ^{1}H NMR (400 MHz, $CDCl_3$): $\delta = 1.014$ (t, 3H, $-CH_3$), 1.543 (m, 2H, H^{13}), 1.58439 (m, 2H, H^{12}), 2.309 (s, 3H, H^2), 4.091 (t, 2H, $-OCH_2-$), 6.951 (d, H, H^6), 7.814 (s, H, H^3), 7.851 (d, H, H^5), 7.972 (d, 2H, H^7, H^{10}), 8.361 (d, 2H, H^8, H^9). IR (in KBr) ν/cm^{-1}: 2931, 2865 (alk. C–H), 3099 (ar. C–H), 1255 (C–O–C), 1592 (N=N), 1526, 1255 (ar. C–N), 860 (N–O).

2.3. Methods and instruments

^{1}H NMR spectra were recorded with the use of a Mercury Plus 400 spectrometer. IR absorption spectra were measured with KBr pellet on a Nicolet Magna FT-IR 460 and UV–vis

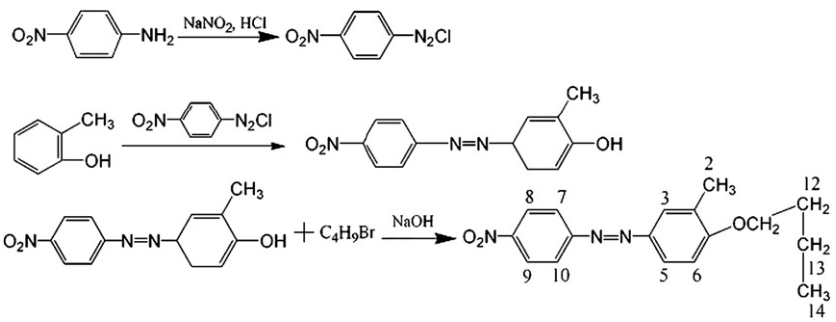

Scheme 1. Synthesis of 1-*n*-butoxy-2-methyl-(4-*p*-nitrophenylazo)benzene.

absorption spectra using a SHIMADZU UV-2450 spectrophotometer. The glass transition temperature of the PR sample was determined via differential scanning calorimeter (DSC) using a Pyris 1 DSC at the heating rate of 10 °C/min. The film thickness and the surface integrity of the film surface were confirmed using a Taly step profilometer (FTSS2-S4 C-3D).

The oxidation/reduction potentials of BMNPAB were measured by cyclic voltammetry (CV). BMNPAB were 1 mM concentration in methylene chloride with tetrabutylammonium-perchlorate (0.1 M). A glassy carbon working electrode and Pt counter electrode were used and the scan rate was 50 mV/S. The potentials were measured against $Ag/AgNO_3$ as reference electrode and each measurement was calibrated as usual with the standard ferrocene/ferrocenium (Fc) redox system. Cyclic voltammograms were recorded on an Autolab PGSTAT30 (ECO Chemie B.V.). The HOMO and LUMO energy values were determined from oxidation and reduction potentials, respectively, by taking the value of −4.8 eV as HOMO energy level for the Fc with respect to zero vacuum level as described by Daub and coworkers [11] in the literature.

2.4. Second-order NLO property

Thin film sample including PVK−10-CdS nanocomposite and BMNPAB was poled by corona poling: a DC 8 kV voltage was applied with a sharp needle electrode at 15 mm to the sample at 80 °C for 2 h and then the sample was cooled to room temperature in the presence of the electric field.

The second harmonic intensity of the poled thin film was determined by a rotational Maker fringe method [12,13]. The fundamental wave of a pulsed Nd:YAG laser (Newwave Tempest 10 Hz) with a pulse width of ∼10 ns was used as the incident light. The output light from the poled sample was passed through a prism to divide the SH wave with 532 nm from the fundamental wave. The SH wave was detected by a monochromator equipped with a photomultiplier (GDB235). The output signal was accumulated by a boxcar integrator (SRS280). All SHG measurements were taken for *mix-p* polarization configuration (*mix-p* denoting a combination of *p*- and *s*-polarized pump radiation with both components equal in magnitude and *p*-polarized SH radiation) in the maker fringe equipment.

2.5. Sample for photoconductivity measurement

PVK and PVK−10-CdS nanocomposite were dissolved in THF and filtered through a 0.2 μm pore size membrane. Thin films (1−2 μm) were fabricated via conventional spin-coating techniques on a glass substrate coated with indium−tin oxide (ITO). Then aluminum counter electrodes were evaporated on the top to form a sandwich device structure. Connecting leads were attached to the aluminum and ITO electrodes with silver conductive epoxy.

Photoconductivity measurement was made using a simple DC photocurrent technique at room temperature in air. Here a voltage was applied to the sample and the current through the sample was measured, both when the sample was illuminated by a He−Ne laser with a wavelength of 632.8 nm and in the dark.

2.6. Polymer nanocomposite device for photorefractivity measurement

PVK−10-CdS nanocomposite (46 mg), 26 mg BMNPAB and 28 mg ECZ were dissolved in 1 ml THF. The solution was subjected to an ultrasonic treatment at 50 kHz for 30 min. Then the solution was spun onto an ITO-glass substrate and dried in an oven at 120 °C overnight. After corona poling, a photorefractive device with PVK−10-CdS:BMNPAB:ECZ = 46:26:28 wt% was fabricated by a second ITO-coated glass slide on top of the first.

The photorefractive measurements were performed using the two-beam coupling (TBC) experiment. Two *p*-polarized beams of intensities 226.3 and 195.4 mW from a Krypton laser with a wavelength of 647.1 nm, having an angle of 20° between them and with their bisector at 50° to the sample normal, were made to intersect within the photorefractive sample.

3. Results and discussion

3.1. Optical properties

An important feature of a photorefractive polymer is its absorption spectrum that determines the wavelength region in which the polymer can be used. The absorption spectrum of the polymer composite is measured as depicted in Fig. 1, the inset shows the absorption spectrum of BMNPAB in acetone and PVK−10-CdS nanocomposite in THF. From previous investigations it is clear that the NLO molecule should not absorb in the interest wavelength region, which can give rise to competing non-photorefractive gratings [14]. In the inset

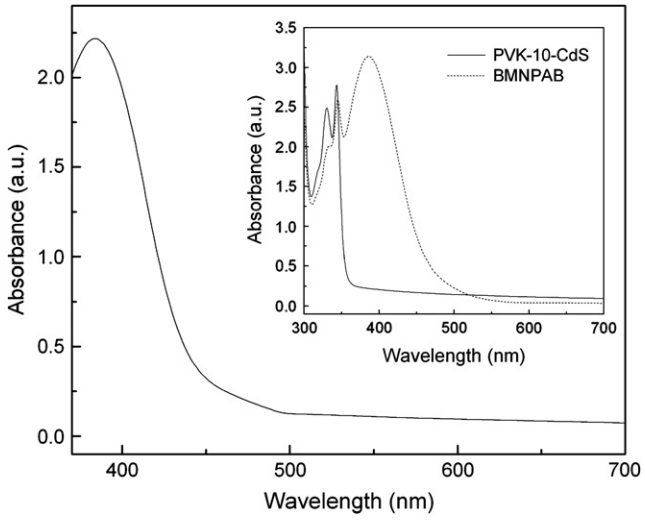

Fig. 1. The recorded UV−vis spectroscopy of a polymer film containing PVK−10-CdS nanocomposite (46 wt%), BMNPAB (26 wt%) and ECZ (28 wt%). The inset shows the absorption spectrum of BMNPAB in acetone (dashed line) and PVK−10-CdS in THF (solid line).

of Fig. 1, it can be observed that BMNPAB has almost no absorption above 600 nm, which contains the typical absorption peaks of the azo ($\lambda_{max} = 389$ nm), while PVK–10-CdS nanocomposite has a little absorption between 400 and 700 nm. Fig. 1 shows the absorption coefficient above 600 nm of the polymer film is very low mainly caused by the absorptions of PVK–10-CdS nanocomposite but not caused by the absorption of BMNPAB. Therefore, the electro-optic and photorefractive characterizations can safely be performed at 647.1 nm.

3.2. Cyclic voltammetry

In order to approximate relative energy level positions, the oxidation/reduction potentials of the chromophore BMNPAB were investigated by cyclic voltammetry. Under the assumption that the energy level of ferrocene/ferrocenium is 4.8 eV below vacuum, the HOMO and LUMO energy values could be calculated according to $E_{HOMO} = -(E_{ox}^{onset} + 4.8)$ eV and $E_{LUMO} = -(E_{re}^{onset} + 4.8)$ eV [15]. As indicated in Fig. 2, the onset oxidation and reduction potentials for BMNPAB, at 0.28 V and −0.93 V (vs. Fc/Fc$^+$), were used to deduce the energy levels of BMNPAB. It was found that the HOMO and LUMO energies for BMNPAB are −5.08 eV and −3.87 eV (vs. vacuum), respectively. Reported [16] value for PVK is oxidized at about 0.77 V (vs. Fc/Fc$^+$) in a chemically irreversible process. So the HOMO level of BMNPAB has greater energy than that of PVK, an electron may be transferred from the BMNPAB to the ionized carbazole group. BMNPAB will act as the hole traps in the PVK matrix or might even perform charge transport themselves.

3.3. Second-order nonlinear coefficient

To reveal the nonlinear optical properties of the polar grating, the second harmonic intensity of the poled thin film sample was investigated in the transmission mode direction using the Maker fringe procedure. The maker fringes recorded from the as-prepared thin films as a function of incidence angle are shown in Fig. 3.

For the thin film sample, the SH intensity $I(2\omega)$ generated by a fundamental light radiation with intensity $I(\omega)$ is given by [17]:

$$I(2\omega) \propto [l_s^2 I^2(\omega) d_{eff}^2 / n^2(\omega) n(2\omega)] \times [\sin^2(\pi l_s/2l_c)/(\pi l_s/2l_c)^2] \quad (1)$$

where l_s is the thin film's thickness, d_{eff} is the measured effective second-order nonlinear optical susceptibility, $n(\omega)$ and $n(2\omega)$ are the index of refraction at frequency ω and 2ω, respectively, and l_c is the coherence length of the thin films. $l_c = \lambda/4[n(\omega) - n(2\omega)]$, is much larger than the thin film's thickness l_s. This yields $[\sin^2(\pi l_s/2l_c)/(\pi l_s/2l_c)^2] \sim 1$. The Y-cut quartz was selected as the referenced sample in order to calculate the second-order nonlinear optical susceptibility of the poled thin film, and the SH intensity of Y-cut quartz was measured under the same test condition.

The result in Fig. 3 shows that the calculated SHG coefficient of 31 pm/V is obtained at 1064 nm in the poled thin film. The poled film also exhibited reasonably thermal and temporal stabilities in their optical nonlinearity. This stability of the nonlinearity allowed us to perform the photorefractive experiments without applying an external electric field.

3.4. Photoconductivity of PVK–CdS nanocomposite

In order to determine whether chemically hybridized CdS nanoparticles can afford the efficient PVK sensitizer, we measured the current–voltage curve of pure PVK and PVK–10-CdS nanocomposite under illumination at excitation wavelengths of 632.8 nm and dark currents including their field dependences as shown in Fig. 4. When the applied

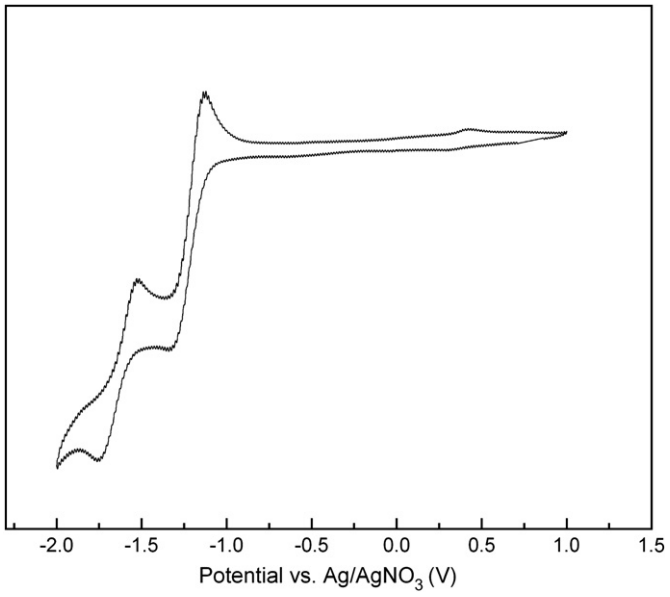

Fig. 2. Cyclic voltammetry curves of BMNPAB measured in acetonitrile at a sweep rate of 50 mV/s.

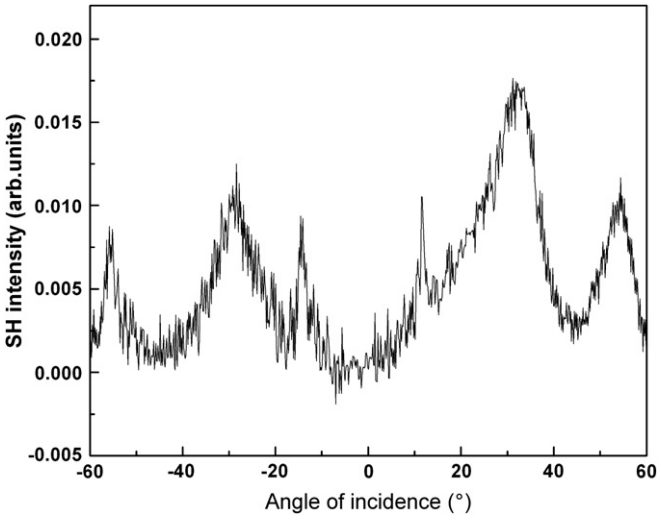

Fig. 3. Maker fringe patterns from the poled film as a function of angle of incidence.

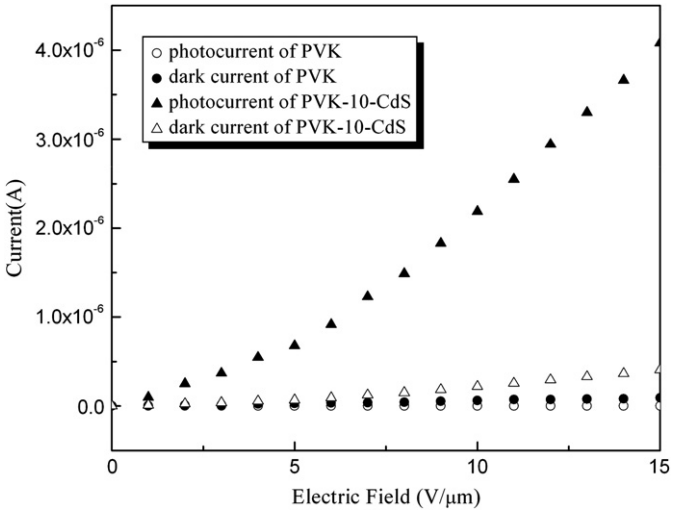

Fig. 4. Photocurrent and dark current–voltage curve of pure PVK and PVK–10-CdS nanocomposite films.

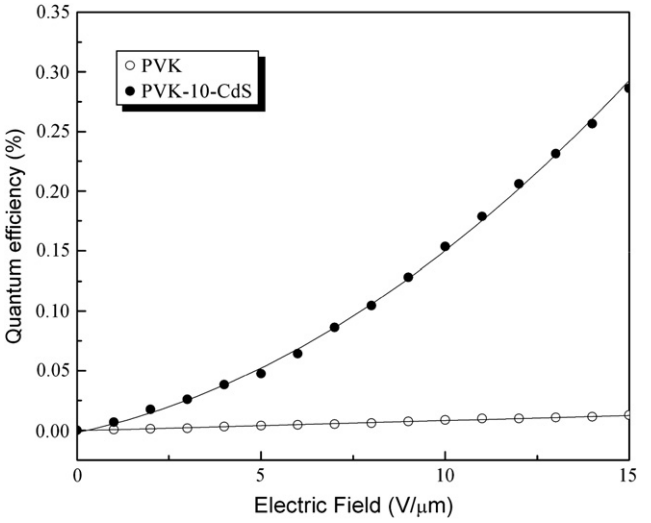

Fig. 5. Photocharge generation quantum efficiency of PVK and PVK–10-CdS nanocomposite films under illumination at excitation wavelengths of 632.8 nm.

electric field was increased, both the photocurrent and dark current increased accordingly. It shows that the photocurrent is increased significantly with the electric field under the illumination when CdS nanoparticles were chemically hybridized in PVK matrix.

Photoconductivity is a convolution of photoinduced charge generation and charge transport. Because a low density of CdS nanoparticles has a small effect on the transport property of the polymer matrix, their main function is the enhancement of the charge generation efficiency. The photocharge generation quantum efficiency (Φ) of PVK–10-CdS nanocomposite can be evaluated from the following equation,

$$\phi(E) = \frac{N_{cc}}{N_{ph}} = J_{ph}\left(\frac{hc}{\lambda e \alpha d}\right) \tag{2}$$

where J_{ph} is the photocurrent density, N_{cc} is the number of charge carriers generated per unit volume, N_{ph} is the number of photons absorbed per unit volume in the sample, h is Planck's constant, c is the speed of light, λ is the wavelength of the incident radiation, e is the fundamental unit charge, α is the absorption coefficient of the sample, and d is the sample thickness. In Fig. 5, the photocharge generation quantum efficiency as a function of applied electric field at 632.8 nm for the PVK and PVK–10-CdS nanocomposite are presented. It has been reported [10] that CdS particles have little contribution in the absorption of the incident light to produce free carriers directly but are mainly responsible for the increased carrier generation efficiency in PVK when the molar ratio of CdS–PVK in the nanocomposites is small. As expected, the results in Fig. 5 show that the PVK–10-CdS nanocomposite exhibits the larger photocharge generation quantum efficiency for the entire range of electric field than that of the PVK film due to the charge carrier transport through the interface between PVK (LUMO level at −2.2 eV) and CdS nanoparticles (LUMO level at −4.8 eV) [9].

3.5. Photorefractive characterization

It is well known the nonlocal nature is the only feature to distinguish PR grating from index gratings caused by other mechanism and thus the asymmetric energy transfer between two writing beams, so-called two-beam coupling is the most direct evidence to confirm the PR effect. The T_g of PVK–10-CdS/BMNPAB/ECZ polymer composite is detected only at 29 °C, so it could be easy to pole at room temperature to achieve the alignment of the chromophore. In TBC experiment, an asymmetric energy transfer between the two coupling beams on the polymer film at a zero external electric field is shown in Fig. 6, the inset shows the experiment performed by chopping one of the two beams and monitoring the transmitted intensity of the other beam. Notice that the intensity

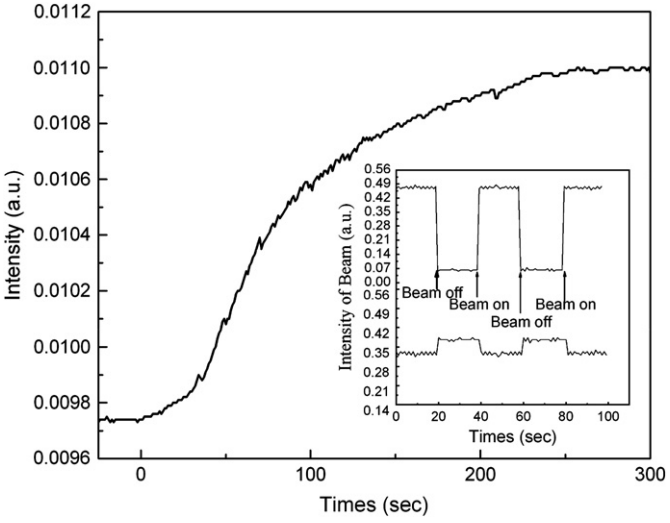

Fig. 6. Asymmetric energy exchange in the 2BC experiment for the sample at zero external field. The inset shows the experiment performed by chopping one of the two beams and monitoring the transmitted intensity of the other beam.

of one beam, as a function of time, kept increasing while that of the other decreasing. When the sample was rotated 180°, the gain and loss beams were also switched, as expected, which is due to reversal of the dipole orientation. These experimental results are clear indications that the grating is due to photorefractive effect and not due to thermal or absorption grating.

The two-beam coupling gain coefficient, Γ, is calculated from the following equation [18]:

$$\Gamma = \frac{1}{L}[\ln(\gamma_0\beta) - \ln(\beta + 1 - \gamma_0)] \quad (3)$$

where the ratio of intensities of the two writing beams before entering the sample is β, L is the thickness of the device, and γ_0 is the ratio of intensities of one writing beam with and without the presence of the other. The diffraction efficiency, η, was measured by blocking one beam after the steady state conditions were reached. According to the equation $\Gamma_{\max} = 2\pi\Delta n/\lambda\cos\theta$, the resulting power oscillations were used to obtain the maximum index modulation (Δn).

The corresponding steady state gain coefficient, diffraction efficiency, maximum index modulation and the properties of the photorefractive polymer composite were presented in Table 1. From a practical point of view, the optical amplification, Γ, must exceed the absorption loss, α, of the photorefractive sample in question. In this case, the net gain coefficient ($\Gamma - \alpha$) of the polymer composite obtained is shown in Table 1.

However, the unique energy exchanges observed in polymer composite is inconsistent with the theoretical and experimental work done so far in the area of PR polymers [15], which predicts the PR performance is strongly dependent on the applied electric field because there is no PR grating without applied electric field and hence no two beam coupling gain. In this study, the possible explanation for the asymmetric two-beam coupling at zero-field may result from the coupling between an internal space-charge field and light-induced orientational grating. And the internal space-charge field seems to play a crucial role.

Firstly, the generation of such an internal space-charge field under a zero external electric field is the injected charges during the corona poling and the dipole orientation of the NLO chromophores [19]. In polymer PR materials, the trapped charges can be much more easily liberated thermally or electrically than those in inorganic PR crystals. If the detrapping rate is large enough, the condition of trap limitation can never be reached and therefore the space-charge field would be a function of photoconductivity. Here, the chemically hybridized PVK–10-CdS nanocomposite exhibits the higher photoconductivity because the better interface between CdS and PVK facilitates fast interfacial carrier transfer and thus increases the charge generation efficiency. And the hole density may transfer to the BMNPAB matrix and a high hole mobility is achieved due to the HOMO of BMNPAB is above that of PVK. In addition, an internal electric field exists that may be generated by chromophore alignment after corona poling, and the optically isotropic of BMNPAB will be removed by causing a partial alignment of the orientationally mobile chromophore resulting in an electric field induced birefringence and a large second-order optical nonlinearity.

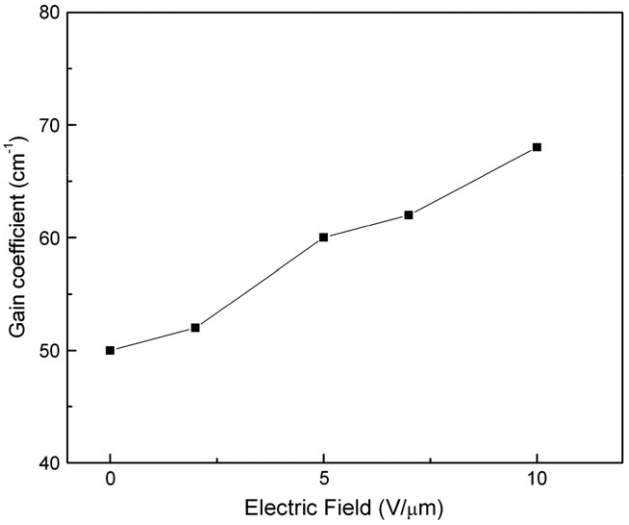

Fig. 7. TBC gain coefficient as a function of applied field.

Secondly, when irradiated by two beams, light-induced orientational effects in azo dyes have suggested rod-like BMNPAB molecules are pumped from the *trans* to the *cis* state with a probability proportional to cos 2(θ) in the presence of polarized light, where θ is the angle between the light polarization direction and the molecular axis [20–22]. After several *trans–cis–trans* cycles, the concentration of the BMNPAB molecules oriented at $\theta = 90°$ is progressively increased and an orientational grating is induced. This photoisomerization may enhance the modulated orientation of the chromophore BMNPAB. Such a light-induced orientational effect has been observed experimentally and explained theoretically in PR polymeric materials [23–25].

We also study the effect of external electric field (E_0) on the photorefractive TBC gain of polymer composite, and the results are presented in Fig. 7. Because the E_0 may enhance the orientation of chromophore and the photoconductivity (e.g. the quantum efficiency and mobility of charge) of materials, the TBC gains increase with the increasing of E_0. When a 10 V/μm external electric field was applied, an optical gain of 68 cm^{-1} was observed.

Table 1
Properties, the gain coefficient and diffraction efficiency of PR polymer system

Polymer composite	Composition (wt%)	Thickness (μm)	α (cm^{-1})	Γ (cm^{-1})	Γ_{net} (cm^{-1})	η (%)	Δn (10^{-3})
PVK–10-CdS/BMNPAB/ECZ	46/26/28	48	22.8	50.0	27.2	4.2	0.48

4. Conclusions

We have demonstrated that the polymer composite including the chemically hybridized PVK–10-CdS nanocomposite, NLO chromophore BMNPAB and plasticizer ECZ, exhibited large photorefractivity. In this system, the poled film containing PVK–10-CdS nanocomposite and BMNPAB exhibited a high SHG coefficient of 31 pm/V, and the stronger internal space-charge field is obtained due to the significant enhancement of photoconductivity in PVK–10-CdS nanocomposite and the dipole orientation of BMNPAB molecules. A net optical gain, of 27.2 cm^{-1} for the polymer composite at a zero external electric field was observed. This result will constitute a significant improvement in the practice application of PR polymer.

Acknowledgements

Key Project of the National Nature Science Foundation of China (no. 60537050) and the Program for Changjiang Scholars and Innovative Research Team in University (PCSIRT, no. IRT0547), Ministry of Education, China are gratefully acknowledged for their financial support.

References

[1] Zhang Y, Cui Y, Prasad PN. Phys Rev B 1992;46:9900–2.
[2] Meerholz K, Volodin BL, Sandalphon Kippelen K, Peyghambarian N. Nature 1994;371:497–500.
[3] Zhang Y, Burzynski R, Ghosal S, Casstevens MK. Adv Mater 1996;8:111–25.
[4] Kippelen B, Peyghambarian N. Adv Polym Sci 2003;161:87–156.
[5] Huang JM, Yang Y, Yang B, Liu SY, Shen JC. Thin Solid Films 1998;327–329:536–40.
[6] Winiaza JG, Zhang LM, Park J, Prasad PN. J Phys Chem B 2002;106:967–70.
[7] Canek FH, Suh DJ, Kippelen B, Marder SR. Appl Phys Lett 2004;85(4):534–6.
[8] Aslam F, Brinks DJ, Rahn MD, West DP, O'Brien P, Pickett N, et al. J Chem Phys 2005;122:184713–6.
[9] Wang S, Yang S, Yang C, Li Z, Wang J, Ge W. J Phys Chem B 2000;104:11853–8.
[10] Yang CL, Wang JN, Ge WK, Wang SH, Cheng JX, Li XY, et al. Appl Phys Lett 2001;78(6):760–2.
[11] Pommerehne J, Vestweber H, Gusws W, Mahrt RF, Bässler H, Porsch M, et al. Adv Mater 1995;7(6):551–4.
[12] Herman WN, Hayden LM. J Opt Soc Am B 1995;12:416–27.
[13] Jerphagnon J, Kurtz SK. J Appl Phys 1970;41:1667–81.
[14] Bolink HJ, Krasnikov VV, Malliaras GG, Hadziioannou G. Adv Mater 1994;6(7–8):574–7.
[15] You W, Wang Q, Wang L, Yu L. Macromolecules 2002;35:4636–45.
[16] Jepsen AG, Wright D, Smith B, Bratcher MS, Declue MS, Siegel JS, et al. Chem Phys Lett 1998;291:553–61.
[17] Shen YR. The principles of nonlinear optics. New York: Wiley; 1984.
[18] Moerner WE, Silence SM. Chem Rev 1994;94:127–55.
[19] Peng ZH, Gharavi AR, Yu LP. Appl Phys Lett 1996;69(26):4002–4.
[20] Sandalphon B, Kippelen N, Peyghambarian, Lyon SR, Padias AB, Hall Jr HK. Opt Lett 1994;19:68–70.
[21] Todorov T, Nikolova L, Tomova N. Appl Opt 1984;23:4309–12.
[22] Sekkat Z, Dumont M. Appl Phys B 1991;53:121–3.
[23] Yu LP, Chen YM, Chan WK, Peng ZH. Appl Phys Lett 1994;64(19):2489–91.
[24] Cheben P, Monte F del, Worsfold DJ, Carlsson DJ, Grover CP, Mackenzie JD. Nature 2000;408:47–64.
[25] Zhang L, Huang MM, Jiang ZW, Yang Z, Chen ZJ, Gong QH, et al. React Funct Polym 2006;66:1404–10.